Title	Variational energy band theory for polarons : mapping polaron structure with the Merrifield method
Author(s)	Zhao, Yang; Brown, David W.; Lindenberg, Katja
Citation	Zhao, Y., Brown, D. W., & Lindenberg, K. (1997). Variational energy band theory for polarons: mapping polaron structure with the Merrifield method. Journal of chemical physics, 106(13), 5622-5630.
Date	1997
URL	http://hdl.handle.net/10220/6731
Rights	

Variational energy band theory for polarons: Mapping polaron structure with the Merrifield method

Yang Zhao[a)]
Department of Physics, University of California, San Diego, La Jolla, California 92093-0354

David W. Brown
Institute for Nonlinear Science, University of California, San Diego, La Jolla, California 92093-0402

Katja Lindenberg
Department of Chemistry and Biochemistry, University of California, San Diego, La Jolla, California 92093-0340

In this paper we revisit from a contemporary perspective a classic problem of polaron theory following the variational approach originally taken by Merrifield. Polaron structure is represented by a variational surface giving the optimal values of the complete set of phonon amplitudes for every value of the joint exciton–phonon crystal momentum κ. Quantities such as complete ground state energy bands (all κ) and effective masses ($\kappa = 0$) are obtained. The parameter space of the problem is mapped, with careful attention given to the self-trapping transition. Through this examination of the complete parameter space at all κ, it is found that the common notion of a sharp self-trapping phenomenon associated with $\kappa = 0$ is a limiting aspect of a more general finite-κ phenomenon. The idea of polaron Wannier states is addressed briefly, and the properties of such states tied to characteristics of the polaron energy band. The successes and failures of the Merrifield method are assessed. © *1997 American Institute of Physics.* [S0021-9606(97)50412-0]

I. INTRODUCTION

In this paper, we revisit from a contemporary perspective a classic problem of polaron theory following the variational approach taken by Merrifield in his 1964 work.[1] Our purpose is several fold: First, computational resources now routinely available make possible a more detailed and comprehensive analysis than was possible at the time of Merrifield's original work. Second, due to the more limited nature of computation and the differing priorities of that time, some questions of interest today were not addressed by Merrifield. Third, though the method is burdened by some serious limitations (that we shall emphasize at appropriate points in our discussion), the method has the benefit of rendering straightforwardly and in high relief some outstanding qualitative features of the polaron landscape that survive generalization to more refined and more accurate methods.

More than a mere updating of Merrifield's work, however, this paper constitutes one ''point'' in a sequence of several increasingly refined variational attacks on a classic problem of polaron theory.[2,3] The Merrifield method is the simplest in the sequence, providing quantitative bounds and qualitative guides for subsequent refinement. The guidance such results provide is both positive and negative; positive in providing a rough picture of polaron structure that can assist in understanding the results of subsequent, more complex variational attacks, negative in highlighting problems with the method that subsequent refinements should remediate. Besides providing increasingly accurate estimates of the ground state energy, sequential refinement in parallel developments should shed light on which features of polaron structure are ''robust'' in that they are resolved with increasing clarity, and which features are artifacts of an insufficiently flexible approach. With this interest in mind, we treat the more limited Merrifield approach with the same scope and respect we give to the more sophisticated methods to be reported separately; here, as there, we shall be particularly concerned with identifying large and small polaron structures, and with assessing the nature of the self-trapping transition.

Though not addressed specifically in this paper, we should note for the reader's perspective that the variational refinements to be reported in subsequent works do not merely increase the number of variational parameters included in computation, but are *qualitative* in relieving what in our estimation are the most significant structural constraints limiting the flexibility of the considered families of trial states. The next ''point'' in the sequence, for example, is the method put forward by Toyozawa[4–6] which, though introduced earlier than that of Merrifield and revisited often since,[7–10] has yet to be implemented with the full scope available in it. The third ''point'' in the sequence is our own generalization of the Toyozawa method,[2,3] including the structure that became of interest during some of our prior studies of the interrelationships between polaron theory and soliton theory.[8–25]

Our central interest in this paper is in the polaron energy band, computed as

$$E^\kappa = \langle \Psi(\kappa) | \hat{H} | \Psi(\kappa) \rangle, \tag{1}$$

wherein κ is the joint crystal momentum label, $|\Psi(\kappa)\rangle$ is an appropriately normalized delocalized trial state, and $\hat{H}$ is the

---

[a)]Present address: Rochester Theory Center for Optical Science and Engineering, University of Rochester, Rochester, New York 14627.

system Hamiltonian. For the latter, we choose perhaps the simplest polaron Hamiltonian, the Holstein Hamiltonian employing optical (Einstein) phonons and local (on-site) exciton–phonon coupling:[26,27]

$$\hat{H} = \hat{H}^{ex} + \hat{H}^{ph} + \hat{H}^{ex-ph}, \tag{2}$$

$$\hat{H}^{ex} = -J \sum_n a_n^\dagger (a_{n+1} + a_{n-1}), \tag{3}$$

$$\hat{H}^{ph} = \omega \sum_n b_n^\dagger b_n, \tag{4}$$

$$\hat{H}^{ex-ph} = g\omega \sum_n a_n^\dagger a_n (b_n^\dagger + b_n), \tag{5}$$

in which $a_n^\dagger$ creates an exciton in the rigid-lattice Wannier state at site n, $b_n^\dagger$ creates a quantum of vibrational energy in the Einstein oscillator at site n, J is the exciton transfer integral between nearest neighbor sites, g is the local coupling strength, and $\hbar = 1$. In momentum space, these several terms take the form

$$\hat{H}^{ex} = \sum_k J_k a_k^\dagger a_k, \tag{6}$$

$$\hat{H}^{ph} = \omega \sum_q b_q^\dagger b_q, \tag{7}$$

$$\hat{H}^{ex-ph} = g\omega N^{-1/2} \sum_{kq} a_{k+q}^\dagger a_k (b_q + b_{-q}^\dagger), \tag{8}$$

wherein $J_k = -2J\cos k$.

Throughout this paper, we use the following Fourier conventions for ladder operators ($c^\dagger = a^\dagger, b^\dagger$) and scalars:

$$c_n^\dagger = N^{-1/2} \sum_p e^{-ipn} c_p^\dagger, \quad c_p^\dagger = N^{-1/2} \sum_n e^{ipn} c_n^\dagger, \tag{9}$$

$$\lambda_n = N^{-1} \sum_q e^{iqn} \lambda_q, \quad \lambda_q = \sum_n e^{-iqn} \lambda_n. \tag{10}$$

To assist in the interpretation of the various formulas to follow, we denote exciton wave vectors by latin k's, phonon wave vectors by latin q's, and reserve the Greek κ for the joint crystal momentum label. In figures, wave vectors are quoted as fractions of π over the lattice constant.

The small polaron trial state may be written as

$$|\Psi(\kappa)\rangle = N^{-1/2} \sum_n e^{i\kappa n} a_n^\dagger \exp\left[-\sum_{n_b} (\beta_{n_b-n}^\kappa b_{n_b}^\dagger \right.$$
$$\left. - \beta_{n_b-n}^{\kappa*} b_{n_b}) \right] |0\rangle, \tag{11}$$

$$|\Psi(\kappa)\rangle = N^{-1/2} \sum_n e^{i\kappa n} a_n^\dagger \exp\left[-N^{-1/2} \sum_q (\beta_q^\kappa e^{-iqn} b_q^\dagger \right.$$
$$\left. - \beta_q^{\kappa*} e^{iqn} b_q) \right] |0\rangle. \tag{12}$$

Though these trial states are delocalized in the sense that they satisfy the appropriate Bloch symmetry condition, and thus any property measured in the ''lab'' frame is uniform over the lattice, the internal structure of these delocalized states is determined by exciton–phonon correlations that are essentially local in character. Here, that local character is such that the electronic component located at site n is associated with a ''phonon cloud'' centered on that site, given by a set of lattice amplitudes $\{\beta_{n_2-n}\}$. The use of a single product coherent state to represent the state of the phonon cloud is significantly limiting in some regimes as we shall see; this cost is mitigated, however, by the qualitative clarity that this central approximation makes possible.

It is easily verified that the above Ansatz state is normalized as given, which contributes to the relative analytical simplicity of the Merrifield treatment. We will work in momentum space to find the phonon amplitudes $\{\beta_q^\kappa\}$ that minimize the variational energy for each κ.

We evaluate the expectation value of the several terms of the Holstein Hamiltonian as

$$\langle \Psi(\kappa)|\hat{H}^{ex}|\Psi(\kappa)\rangle = -J(e^{i\kappa} S_{+1}^{\kappa*} + e^{-i\kappa} S_{-1}^\kappa), \tag{13}$$

$$\langle \Psi(\kappa)|\hat{H}^{ph}|\Psi(\kappa)\rangle = N^{-1} \sum_q |\beta_q^\kappa|^2, \tag{14}$$

$$\langle \Psi(\kappa)|\hat{H}^{ex-ph}|\Psi(\kappa)\rangle = -N^{-1} g\omega \sum_q (\beta_{-q}^{\kappa*} + \beta_q^\kappa), \tag{15}$$

wherein S_n^κ is the Debye–Waller factor,

$$S_n^\kappa = \exp\left[N^{-1} \sum_q |\beta_q^\kappa|^2 (e^{iqn} - 1) \right]. \tag{16}$$

Minimization of E^κ with respect to $\beta_q^{\kappa*}$ leads to the self-consistency equations for β_q^κ:

$$\beta_q^\kappa = \frac{g}{1 - 4JS^\kappa \sin(\kappa - \Phi^\kappa - q/2)\sin(q/2)}, \tag{17}$$

$$S^\kappa = \exp\left[N^{-1} \sum_q |\beta_q^\kappa|^2 (\cos q - 1) \right], \tag{18}$$

$$\Phi^\kappa = N^{-1} \sum_q |\beta_q^\kappa|^2 \sin q, \tag{19}$$

where S^κ and Φ^κ are the magnitude and the phase of the complex Debye–Waller factor $S_{\pm 1}^\kappa$. This shows the optimal β_q^κ to be real, and establishes the ''sum rule,''

$$\sum_n \beta_n^\kappa = \beta_{q=0}^\kappa = g. \tag{20}$$

It is worth noting that Φ^κ can be nonzero only if the distribution of optimal phonon amplitudes displays certain asymmetries with respect to the phonon wave vector; i.e.,

Φ^κ vanishes if $\beta_q^\kappa = \beta_{-q}^\kappa$ or if $\beta_q^\kappa = \beta_{q\pm\pi}^\kappa$. It has been nearly universal in variational calculations of polaron band structures to assume $\beta_q^\kappa = \beta_{-q}^\kappa$ at some point prior to numerical computation; however, one can show that this symmetry applies strictly only at $\kappa = 0, \pm\pi$. At intermediate κ, the β_q^κ satisfy neither of these symmetries precisely, with the result that Φ^κ generally rises from and returns to zero as κ ranges from 0 to π.

Replacing the summations in Eqs. (18) and (19) with integrations and carrying out the integrations under the assumption of an infinite lattice ($N \rightarrow \infty$) we arrive at the self-consistency equations first obtained by Merrifield:

$$S^\kappa = \exp(-g^2 \Delta^\kappa), \tag{21}$$

$$\Phi^\kappa = -2Jg^2 \Delta^\kappa S^\kappa \sin(\Phi^\kappa - \kappa), \tag{22}$$

and

$$\Delta^\kappa = \left[\frac{1}{\sqrt{[1 + 2JS^\kappa \cos(\Phi^\kappa - \kappa)]^2 - (2JS^\kappa)^2}} \right]^3. \tag{23}$$

It can be shown that S^κ and Δ^κ are even and Φ^κ odd in κ. With the further aid of the integral relations

$$\frac{1}{2\pi} \int_0^{2\pi} dq \frac{1}{1 - 4JS^\kappa \sin(\kappa - \Phi^\kappa - q/2)\sin(q/2)} = [\Delta^\kappa]^{1/3}, \tag{24}$$

$$\frac{1}{2\pi} \int_0^{2\pi} dq \frac{1}{[1 - 4JS^\kappa \sin(\kappa - \Phi^\kappa - q/2)\sin(q/2)]^2}$$
$$= \Delta^\kappa [1 - 2JS^\kappa \cos(\kappa - \Phi^\kappa)], \tag{25}$$

we then obtain the energy–momentum relation:

$$E^\kappa = g^2(\Delta^\kappa - 2[\Delta^\kappa]^{1/3}) - 2JS^\kappa(1 - g^2\Delta^\kappa)\cos(\kappa - \Phi^\kappa). \tag{26}$$

The self-consistency equations (21)–(23) can be solved by numerical iterative techniques. Solutions may be given in various forms, depending on the purpose to which they are to be put. For example, the least redundant form of solution consists of the $2N$ parameters $\{S^\kappa, \Phi^\kappa\}$, from which all other quantities can be computed; however, the set of N^2 phonon amplitudes $\{\beta_q^\kappa\}$ is in some respects more useful despite its high redundancy. The dependence of β_q^κ on q, for example, is in inverse Fourier relation to the spread of the ''phonon cloud'' in real space, so a ''flatter'' q dependence implies a more compact lattice distortion, and a more distorted (nonsinusoidal) q dependence implies a lattice distortion with significant amplitude beyond nearest neighbors. Thus the set $\{\beta_q^\kappa\}$ is useful in characterizing polaron structures and for making comparison with results of other variational approaches that cannot be reduced to a small number of parameters.

Figure 1 shows both representations of a particular solution in the nonadiabatic regime. In this example, the small amplitude of the variations of β_q^κ with respect to the mean implies that most of the lattice distortion is concentrated on one site, and the nearly sinusoidal shape of the undulation implies that most of the remaining lattice distortion is limited
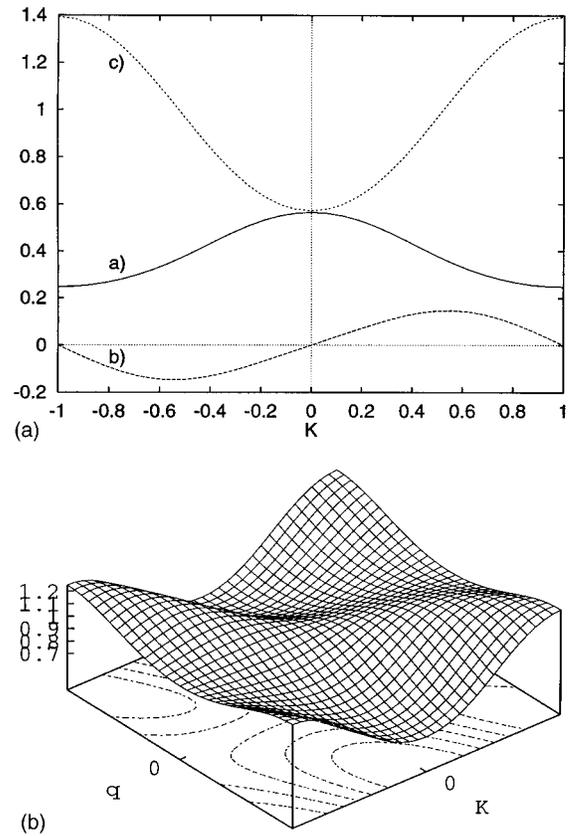

FIG. 1. (a) Variational parameters S^κ (solid line), Φ^κ (dashed line), and $g^2\Delta^\kappa$ (dotted line) for $g = 1, J = 0.2$. (b) β_q^κ representation of the same solution.

to the immediately adjacent sites. With increasing coupling strength, the amplitude of this undulation decreases while its shape becomes increasingly sinusoidal, corresponding to a contraction of the lattice distortion down to a single site in the strong coupling limit. This shape of the $\{\beta_q^\kappa\}$ surface and this trend with changes in coupling strength is characteristic of the entire small polaron regime.

At general κ, the undulation of β_q^κ does not satisfy either of the symmetries that allow Φ^κ to vanish, implying a nontrivial, if weak, involvement of phonon momenta in the structure of the polaron states.

The Debye–Waller factor S^κ (see Fig. 1) reaches a minimum at $|\kappa| = \pi$, reflecting the fact that the higher-lying states nearer the Brillouin zone edge interact more strongly with the nearby one-phonon continuum, resulting in stronger band compression near the zone boundary. This increase in exciton–phonon interaction with increasing κ is reflected in the corresponding β_q^κ surface as an increase in the mean phonon amplitude with κ. This mean amplitude, through the Fourier relationship, Eq. (10), is the real-space amplitude at the center of the phonon cloud, and is given through Eq. (24) as $\beta_{n=0}^\kappa = g[\Delta^\kappa]^{1/3}$. This quantity is smaller at the Brillouin zone center than at the zone boundary, as indicated by

$$\beta_{n=0}^{\kappa=0} = \frac{g}{\sqrt{1 + 4JS^{\kappa=0}}}, \quad \beta_{n=0}^{\kappa=\pm\pi} = \frac{g}{\sqrt{1 - 4JS^{\kappa=\pm\pi}}}. \tag{27}$$

This, together with the sum rule requiring that the sum of all real-space phonon amplitudes equal the dimensionless coupling constant g, shows that there must be a compensating decrease in the net of all phonon amplitudes away from the center of the phonon cloud. These trends are consistent with the notion of a polaron that grows more compact with increasing κ; however, in view of the fact that real-space phonon amplitudes may be negative and even complex, such an inference cannot be made on this basis alone. The sense in which polaron states *do*, in fact, grow more compact with increasing κ is reflected in specific results in the sections that follow.

II. LIMITING BEHAVIOR: SMALL *J*, FINITE *g*

In the absence of any interaction between an exciton and phonon system, i.e. when $g=0$, the adiabaticity of the juxtaposed systems can be quantified by a ratio of electronic and vibrational time scales such as $4J/\hbar\omega$, or, as in our scaling, simply $4J$; a large value of this ratio characterizes an *adiabatic* situation in which electronic dynamics evolves significantly faster than vibrational dynamics, and a small value characterizes the *nonadiabatic* situation in which electronic dynamics is comparatively slow. This notion of adiabaticity attaches to the *bare* exciton, and though most clearly evident in the absence of any exciton–phonon coupling, the adiabaticity ratio is one of the two control parameters that discriminate between distinct polaron structures.

Less easily characterized but often of more direct physical interest is a notion of adiabaticity that attaches to the *dressed* exciton, or polaron. The time scales of dressed transport are expected to be lengthened relative to bare transport, sometimes dramatically, and are often taken to be characterized by the product of the bare transfer integral and a Debye–Waller factor. Though the relationship between real polaron time scales and an effective, reduced transfer integral is complicated [see Eq. (26)], the Merrifield method supports the notion as being sound in a broadly significant way. Considering the fact that the bare transfer integral J appears self-consistently *only* as a product with the Debye–Waller factor S^κ, assorted quantities of interest can be expanded to low order in the parameter JS^κ and leading dependences determined. For example, to leading order in JS^κ,

$$S^\kappa = e^{-g^2}, \quad E^\kappa = -g^2 - 2Je^{-g^2}\cos\kappa, \quad m_{\text{eff}} = m_0 e^{g^2},$$
(28)

consistent with the expected properties of small polarons, including the exact $J=0$ limit. Although the ''bare'' adiabaticity condition $4J \ll 1$ is sufficient to arrive at this result, the self-consistent result is much stronger since the *reduced* transfer integral JS^κ may be small even for large J provided the exciton–phonon coupling is sufficiently strong.

While this picture is no doubt valid at least in a limiting sense, one must be cautious against over-interpretation; though the above considerations leave little question that small polaron states exist over a substantial regime of the problem, this in itself says nothing about the uniqueness of these states at finite JS^κ, and when not unique, whether small polaron states are associated with the relevant global energy minimum. In fact, a distinct class of states exists over a large regime of the problem, and these *coexist* with small polaron states in a nontrivial overlapping regime. The notion of a *self-trapping transition* between small polaron states and large polaron states takes shape in this regime of coexistence and is addressed in some detail in section IV.

III. LIMITING BEHAVIOR: SMALL *g*, FINITE *J*

Consider the joint electron–phonon eigenstates of the Holstein Hamiltonian when $g=0$. These states can be labelled $n+1$-tuples $\{\kappa, q_1, \ldots, q_n\}$ wherein κ is the total crystal momentum as elsewhere in this paper, n is the number of phonon quanta present, and q_i is the wave vector of the ith phonon quantum. When $4J < 1$, the states containing zero phonon quanta ($\{\kappa\}$) have the lowest energy for all κ; however, when $4J > 1$, some higher-lying zero-phonon states have energies higher than some states of the same κ containing one or more phonons; i.e., the bare exciton band penetrates the one-phonon continuum that begins at $E(0) + \hbar\omega$. This implies that these higher-lying zero-phonon states are *unstable* to decays into one- or multi-phonon states in the presence of exciton–phonon interactions, and suggests that polaron eigenstates and energy bands in the adiabatic regime ($4J > 1$) may differ significantly in character from those of the nonadiabatic regime ($4J < 1$).

The small-J or nonadiabatic case is relatively simple since the lowest energy band consists of zero-phonon states for all κ when $g=0$. In this case, turning on the exciton–phonon coupling only gradually deforms the polaron band from the unperturbed exciton band, reflecting the more or less gradual formation of the virtual phonon cloud around the electron. With increasing coupling strength, these states smoothly deform into the familiar small polaron states. The results displayed in Fig. 1 correspond to such a nonadiabatic case.

When $g=0$, provided only that $4J > 1$, there exists a κ_c determined by the relation $2J(1-\cos\kappa_c) = 1$ such that

$$|\Psi(\kappa)\rangle = a^\dagger_{k=\kappa}|0\rangle, \quad \text{for } |\kappa| < \kappa_c,$$
(29)

$$|\Psi(\kappa)\rangle = b^\dagger_{q=\kappa}a^\dagger_{k=0}|0\rangle, \quad \text{for } |\kappa| > \kappa_c,$$
(30)

the former being a zero-phonon state in which the exciton carries all the crystal momentum, and the latter being a state in which the exciton is at rest and all the crystal momentum is carried by a single free phonon quantum. The latter state is not well approximated by a small polaron Ansatz due to the number-indefinite character of the coherent state used to represent the lattice component. This inherent structural misfit can result in large gaps between the variational estimate of the energy band and the exact ground state, as is seen in Fig. 2. For $|\kappa| < \kappa_c$, the variational band coincides with the zero-phonon band as it should; however, for $|\kappa| > \kappa_c$, the variational band deviates strongly from the target value of $E(\kappa) = -1$. Since we understand the source of this error, and therefore can be guided toward its repair, we can be encouraged that despite being far removed from the single quantum character of the target state, the lattice coherent state does a
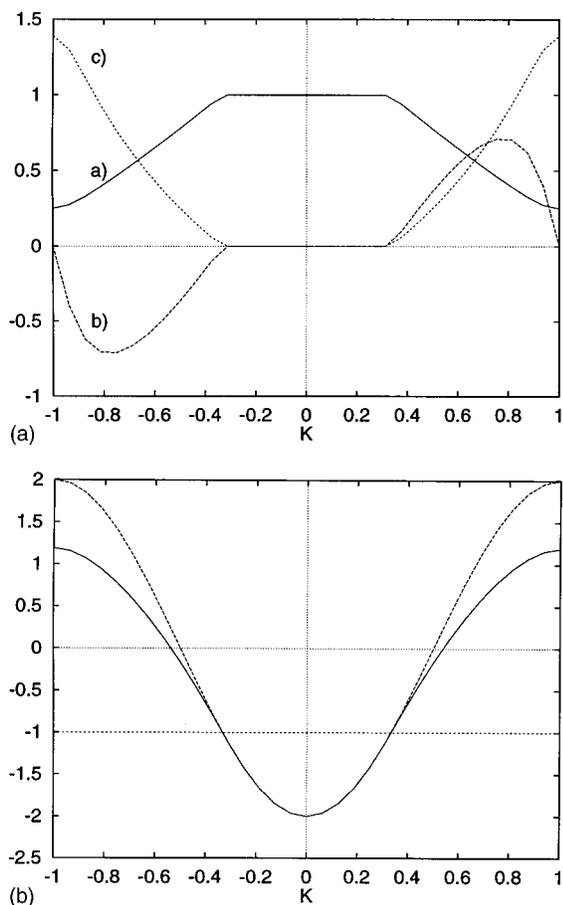
FIG. 3. Phase diagram. The upper portion of the diagram is populated by variational solutions that are small-polaron-like at all κ. The lower portion of the diagram is populated by variational solutions that are large-polaron-like at all κ. The wedge-shaped transition region is populated by variational solutions that are large-polaron-like below some κ^*, and small-polaron-like above this κ^*. The "critical point" is given approximately by $J_c = 0.89, g_c = 1.90$. The points marked explicitly correspond to the locations of the several variational solutions for β_q^κ shown in Figs. 1, 2, 5, and 6.

FIG. 2. (a) S^κ(solid line), Φ^κ (dashed line), and $g^2 \Delta^\kappa$ (dotted line) for $g = 0.01, J = 1$; $\kappa_c = \pi/3$. (A finite value of g is necessary in order to compute optimal solutions consistent with the limit $g \rightarrow 0^+$.) (b) Comparison between the $J = 1$ bare band (dashed) and the variational band for $g = 0.01, J = 1$ (solid line). The horizontal (dotted) line at $E = -1$ indicates the lower bound of the phonon continuum and the exact value of $E(\kappa)$ for $|\kappa| > \kappa_c$. The crystal momentum κ is scaled by π.

respectable job of simulating such a state by concentrating the variational amplitudes β_q^κ in a sharp distribution centered near the line $q = \kappa$.

IV. PHASE DIAGRAM

Because we expect to find qualitatively distinct polaron structures in different regimes of the problem, one desirable result of studies such as ours is a phase diagram that in some useful way maps the system parameter space. One would expect the principal feature of such a phase diagram to be a boundary line separating a small polaron region from a large polaron region; such a line would be expected to be associated with the common notion of a more-or-less sharp self-trapping transition. Though on formal grounds the self-trapping transition is expected to be smooth,[28–31] it is commonplace for approximate treatments such as ours to encounter discontinuities where the polaron structure changes too rapidly to be represented accurately. While such discontinuities must be understood to be artifacts of an insufficiently flexible method, they are also convenient "mark-
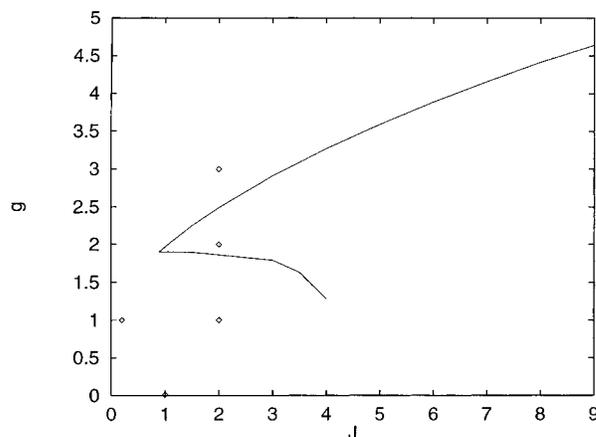
ers" identifying the location of critical points on the phase diagram. In view of the limited scope of the Merrifield method, we shall pay attention to self-trapping-related discontinuities in this latter respect; we shall find that the qualitative features of self-trapping thus revealed persist significantly when more accurate methods are applied and the discontinuities largely "healed."

Variational solutions in the form of an energy band and a complete set of Bloch states $\{E^\kappa, |\Psi(\kappa)\rangle\}$ can be obtained numerically for essentially any system parameters J and g. These solutions are found to smoothly follow incremental changes in the control parameters J and g over most of the phase diagram with, however, dramatic exception in a wedge-shaped region at moderate to large values of J and g (see Fig. 3). The nature of the exception is such that at every point within the wedge-shaped region there exists a κ^*, the particular value of which is dependent upon J and g, at which the variational energy band $E(\kappa)$ is not smooth. More specifically, the variational solutions in a neighborhood around κ^* are not unique, such that the family of solutions continuous with unique solutions at high κ cease to be the minimum energy solutions below κ^*, and the family of solutions continuous with unique solutions at low κ cease to be the minimum energy solutions above κ^* (see Fig. 4). In such cases, the states above κ^* can be meaningfully interpreted as small polaron states, and the states below κ^* can be interpreted as large polaron states, and the "event" marked by κ^* can be understood as a κ-dependent self-trapping transition at fixed J and g.

The usual notion of a self-trapping transition is associated with discrete changes in properties of the $\kappa = 0$ state as J and/or g are varied; for example, with effective mass, whose rapid change or jump is the traditional hallmark of self-trapping. Such discrete behavior yields a self-trapping
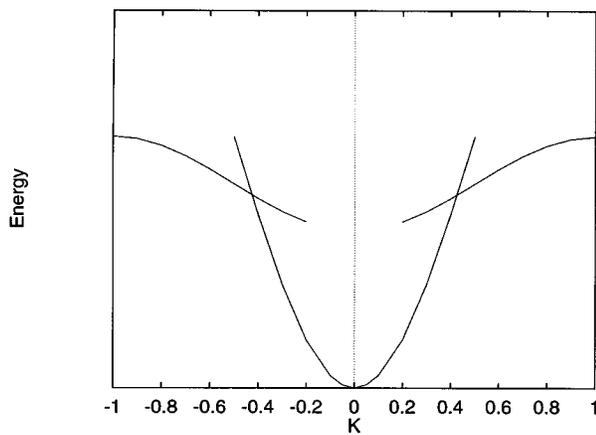
FIG. 4. Schematic illustration of the typical variational situation in the transition region. Two distinct classes of stable solutions exist, and *coexist* over a limited range of κ. The variational energy band is arrived at by discarding the higher-energy solutions and joining the resulting branches at their intersection. $K = \kappa/\pi$.

FIG. 5. β_q^κ at $J = 2$ for three different values of g. (a) $g = 3$, unique solution in the small-polaron regime. (b) $g = 2$, mixed solution characteristic of the transition region. (c) $g = 1$, unique solution in the large-polaron regime. Note the differences in scale.

"line" in parameter space separating large and small polaron structures. The κ-dependent self-trapping transition we observe, though discrete, is discrete in a different way; since κ^*'s exist over a range of J and g, there is not a single transition line, but a transition *region* within which the transition *moves* through the band. At every point in this region, the band is interpretable as large-polaron-like at small κ, and small-polaron-like at large κ. The usual notion of a self-trapping transition is recovered, however, if from any point within the transition region, the coupling parameter is increased sufficiently. In response to increasing coupling strength, κ^* moves toward the center of the Brillouin zone, such that $\kappa^* \to 0$ at some finite g. At this point, the $\kappa = 0$ solution changes abruptly from being of large polaron character to small polaron character, with properties such as the effective mass experiencing the discrete changes one would expect.

To clarify how this transition can be at once sharp in κ but broad in J and/or g (or vice versa), we show in Fig. 5 three optimal β_q^κ surfaces representing a transit from weak to strong coupling at fixed J in the adiabatic regime; note that each β_q^κ surface is plotted to a different scale, and that $\kappa_c \approx 0.23\pi$.

The $(J, g) = (2, 1)$ surface is typical of "large polaron" solutions at weak coupling where such solutions are unique. These solutions are characterized by three qualitative features: Below κ_c, phonon amplitudes are nearly symmetric in q (momentum-poor) and fall off in a smooth, pulse-like fashion as q ranges from the zone center to the zone edge, reflecting a pulse-like lattice distortion spanning many lattice sites as is typical of large polarons. Above κ_c, phonon amplitudes are strongly asymmetric in q (momentum-rich), imperfectly reflecting the strong one-phonon character of the target solutions at weak coupling as previously discussed; continued lowering of g from this value would see this asymmetric component narrow toward an arc of delta-functions near the $q = \kappa$ line. At highest κ, near the Brillouin
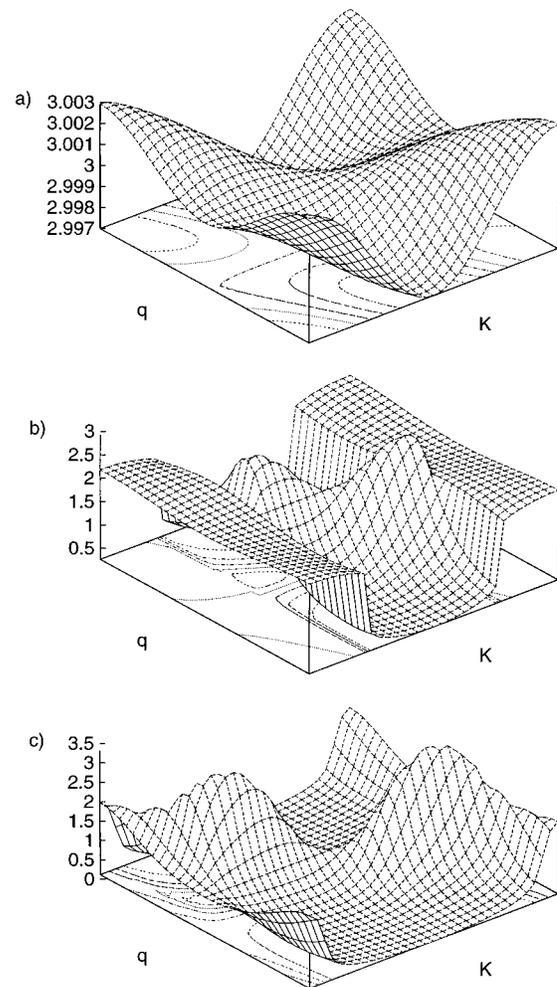
zone boundary, phonon amplitudes again become nearly symmetric in q (momentum-poor) with a mean value significantly greater than at the Brillouin zone center; this reflects a significant contraction of the lattice distortion in real space, and in respects is more suggestive of a small polaron structure.

The $(J, g) = (2, 3)$ surface is typical of "small polaron" solutions at strong coupling where such solutions are unique. These solutions are characterized by weak undulations around a mean value reflecting a momentum-poor phonon cloud and a lattice distortion highly localized in real space.

The $(J, g) = (2, 2)$ surface is typical of the transition region; the obvious discontinuity marks the location of κ^* for these parameters. The low-κ portion of the surface is strikingly similar to the large polaron surface at weak coupling, and the high-κ surface is strikingly similar to the small polaron surface at strong coupling.

As one varies parameters so as to cross the transition region, say from weak to strong coupling at fixed J, the discontinuity marked by κ^* *moves* toward the zone center,
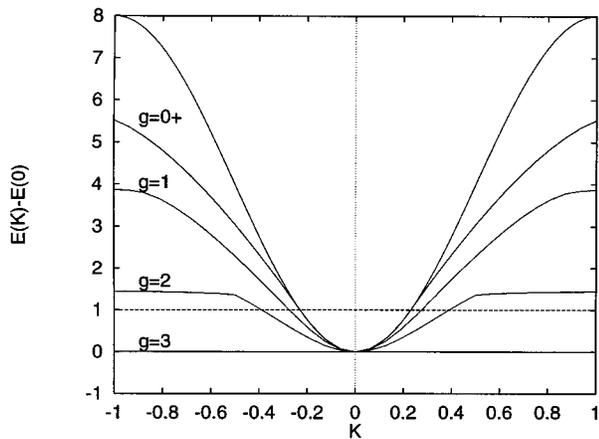
FIG. 6. Polaron energy bands for $J=2$, shifted by the ground state energy: $E(\kappa)-E(0)$. The uppermost curve corresponds to the rigid-lattice energy band, and the curves below it, from top to bottom, represent variational energy bands for $g=0^+,1,2,3$. The last of these energy bands appears flat since its bandwidth of less than 10^{-3} is considerably below the resolution of the figure. The dashed line indicates the lower boundary of the one-phonon continuum.

FIG. 7. The ratio of the polaron effective mass to the bare exciton mass (m_{eff}/m_0) is plotted against electron–phonon coupling in logarithmic scale for several different values of the transfer integral. The uppermost curve corresponds to the limiting dependence of the polaron effective mass upon the coupling constant in the limit $J\rightarrow 0$. The remaining curves, from top to bottom, correspond to the cases $J=0.5$, $J=1$, and $J=2$.

consuming the large polaron fraction of the variational solutions until finally, at the traditional self-trapping line, only small polaron contributions remain.

For values of J less than the ''critical value'' J_c, it is still the case that solutions are ''large-polaron-like'' at weak coupling, and ''small-polaron-like'' at strong coupling; however, the transition between these two occurs smoothly. In fact, as one moves away from the critical point toward lower J's, and particularly the nonadiabatic regime where $4J<1$, the distinctions rendered so strongly in Fig. 5 are barely evident.

The energy bands associated with the several examples in Fig. 5 are shown in Fig. 6 together with the rigid-lattice energy band and the $g=0^+$ variational energy band for comparison. In this particular representation, we have subtracted out the ground state energy so that all of the displayed bands are aligned at $\kappa=0$, showing how the *shape* of the energy band changes with increasing coupling strength. Owing to the dramatic narrowing of the polaron band that occurs with increasing coupling strength, the band in the $g=3$ case varies by approximately 10^{-3} between $\kappa=0$ and $\kappa=\pm\pi$ and is thus indistinguishable from a flat line on the scale shown; on an appropriate scale, however, such strongly-compressed bands associated with small polarons are found to be nearly indistinguishable from the ''ideal'' form $2Je^{-g^2}(1-\cos\kappa)$.

The most outstanding feature of this energy band comparison highlights one of the outstanding failures of the Merrifield method; that is, the gross over-estimation of the ground state energy for $|\kappa|>\kappa_c$. As has been discussed earlier, such errors are to be expected in the weak coupling regime; however, this comparison shows that the errors continue to be significant at coupling strengths that may be considered at least moderate on an absolute scale. This inherent quantitative difficulty with the method tends to obscure the more qualitative and more important feature of the energy
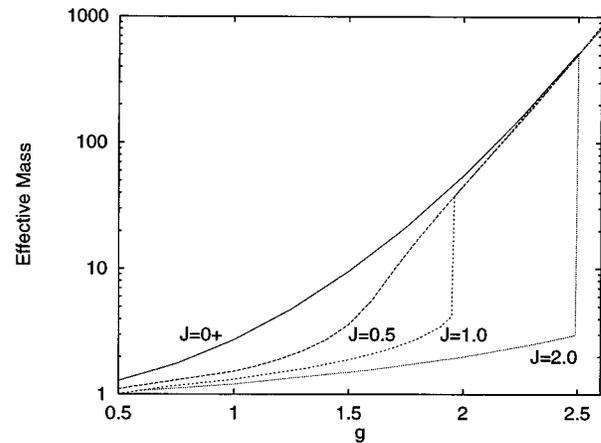
band comparison, and that is that consistent with the segregation of the phonon amplitudes β_q^κ into small-polaron-like and large-polaron-like sets above and below some κ^*, the high-κ portion of the polaron energy band tends to be more flat and more responsive to increasing exciton phonon coupling than the low-κ portion, up to the conventional self-trapping transition. Above the self-trapping transition, the distinguishable low-κ, large-polaron-like region ceases to exist, and the polaron band appears essentially uniformly narrowed across the entire Brillouin zone.

These trends are reflected to a lesser degree in the polaron effective mass, which we compute according to

$$\frac{m_{\mathrm{eff}}}{m_0}=\frac{2J}{\partial^2 E^\kappa/\partial\kappa^2|_{\kappa=0}}. \tag{31}$$

While Eq. (26) can be manipulated to yield one or another formula for the effective mass in terms of J, g, and some variational quantity such as the Debye–Waller factor $S^{\kappa=0}$, less cumbersome and more revealing is a composite illustration such as Fig. 7. For weak exciton–phonon coupling at any value of the transfer integral J, the polaron mass approaches that of the bare exciton. On the other hand, with increasing exciton–phonon coupling, the polaron mass grows monotonically without bound. This increase in the effective mass has several characteristic features. The first is the fact that the growth in the effective mass at weak coupling is slower for larger transfer integrals J; this is one aspect of adiabaticity, that the more mobile excitons are less easily and less completely ''clothed'' by the phonon cloud, and it may be said that this trend in the effective mass is characteristic of large polarons. For any particular value of the transfer integral, however, at sufficiently large coupling the growth in the effective mass follows a single, strong dependence on the exciton–phonon coupling characteristic of small polarons. The ''transition'' between these characteristic behaviors is smooth or abrupt depending on whether the

exciton transfer integral J is, respectively, below or above the critical value J_c; here, $J_c = 0.89$, so that the transition is smooth for $J = 0.5$ and abrupt for $J = 1$ and $J = 2$.

V. WANNIER STATES

In a straightforward tight-binding approach such as ours, the rigid-lattice electronic Bloch states $\{|k\rangle\}$ of a particular band are related the rigid-lattice Wannier states $\{|n\rangle\}$ of that band through a Fourier transform in k and n.[32–35] Similarly, in deformable lattices, there should exist site-localized states associated with polaron energy bands that reflect the local character of the polaron.[36,37] We may construct such states by Fourier transforming polaron Bloch states in κ and n,

$$|\Phi(n)\rangle = \frac{1}{\sqrt{N}} \sum_\kappa \exp(-i\kappa n)|\Psi(\kappa)\rangle. \tag{32}$$

In view of the inherent redundancy of Wannier states, we may focus on $n = 0$. This transformation does *not* generally recover the rigid-lattice Wannier state $|n\rangle$, because of the κ-dependence of the phonon amplitudes β_q^κ.

While we may think of polaron Wannier states as being the states created by polaron operators in the site representation; e.g.,

$$|\Phi(0)\rangle = A_{n=0}^\dagger |0\rangle, \tag{33}$$

an important characteristic of Wannier states is the degree to which the *bare* exciton density within them is localized. Perhaps the simplest objective measure of this property is the variance of the exciton density, defined as

$$\langle n^2 \rangle = \langle \Phi(0)| \sum_n n^2 a_n^\dagger a_n |\Phi(0)\rangle, \tag{34}$$

where, without loss of generality, we have chosen the polaron Wannier state associated with the origin. Using the Merrifield Ansatz state, one may show that

$$\langle n^2 \rangle = \frac{1}{N^2} \sum_{\kappa q} \left(\frac{\partial \beta_q^\kappa}{\partial \kappa} \right)^2. \tag{35}$$

The spread of the exciton density is thus shown to be an average over all total crystal momenta κ and all phonon wave vectors q of positive-definite quantities. Those quantities are squares of the local rates of change of the variational phonon amplitudes β_q^κ with respect to the total crystal momentum. That is, the spread of the exciton density is not given directly by the magnitudes of the phonon amplitudes, but by an aggregate measure of the κ-dependent distortion of the sheet of variational phonon amplitudes.

With this result, together with the variational results collected in this paper, we may qualitatively characterize local polaron structure in various regimes. For example, at small J and/or large g (small polaron regime), where β_q^κ is characterized by smooth, weak undulations about a mean value, the exciton density is compact, spreading with increasing J or decreasing g. At large J and small g (large polaron regime), where β_q^κ is characterized by smooth but strong excursions in the vicinity of the $\kappa = q$ line, the exciton density is broad, spreading with increasing J or decreasing g.

In the transition region, the β_q^κ that result from our variational calculation are not smooth with respect to κ, carrying the physically unlikely implication that the exciton density has no second moment in that part of the phase diagram; this is one of many manifestations of the discontinuous nature of the self-trapping transition that underscores the need to exercise care in its interpretation.

Considering the relationship between the phonon amplitudes and the polaron energy band, these findings suggest a general relationship may exist between the spread of the exciton density in the polaron Wannier state and the κ-dependence of the energy band distortion. Such a relationship could offer direct linkage between certain experimental observables such as optical lineshapes and much more elusive local properties.

VI. CONCLUSIONS

In this paper we have examined the polaron problem as constituted in the Holstein Hamiltonian following the variational approach originally taken by Merrifield.[1] This method offers many analytical, computational, and interpretive advantages at the cost of admitting certain artifacts that limit its usefulness as a quantitative tool. Our purpose, however, has not been to employ this method and its results as ends in themselves, but to expand upon Merrifield's original work, analyze its results from a contemporary viewpoint, and establish a suite of results that may guide subsequent refinement of the method and can be used as standards against which the qualitative and quantitative merits of such refinements may be judged.

The Merrifield method is straightforwardly implemented, its solutions simply rendered and readily interpreted. Unlike methods which focus on long wavelengths, this approach yields variational polaron energy bands and the associated Bloch states at all κ, and unlike perturbative methods, results obtain (with varying quality) over essentially all of the system parameter space. Since the structure of each polaron Bloch state can be "exploded" and viewed in the form of a full set of phonon amplitudes, the structure of the phonon cloud can be assessed for all κ and essentially all system parameters. In this way a phase diagram of a polaron structure can be developed, on which can be located such important features as the self-trapping transition. Through such an exercise, however, we have found that the usual notion of a self-trapping transition at $\kappa = 0$ is a limiting aspect of a more general self-trapping phenomenon occurring over a range of κ (*including* $\kappa = 0$) and over a more-or-less broad region of parameter space. This finding shows how polaron bands may be large-polaron-like at long-wavelengths ($|\kappa|$ less than some κ^*) and small-polaron-like at short-wavelengths. This points to the notion of self-trapping as being a *dynamic* as well as a static phenomenon, occurring not only through changes in system parameters, but in appropriate parameter regimes occurring also in response to applied fields that produce changes in κ.

The virtues of the Merrifield method are offset in respects by some dramatic shortcomings. Self-trapping-related discontinuities are rampant. Though we can understand the phenomena marked by such discontinuities and appreciate the qualitative information contained in them, the fact of their existence points to uncontrolled quantitative inaccuracies in those regimes where they occur. While such difficulties associated with self-trapping are found at moderate to strong coupling, there are also outstanding problems at weak coupling, at least in the adiabatic regime ($4J>1$) where the variational energy band grossly overestimates the ground state energy at higher momenta ($|\kappa|>\kappa_c$). This difficulty extends at least to intermediate coupling, underscoring the fact that the quality of the variational estimates is nonuniform both across the energy band and across the system parameter space.

Such difficulties are perhaps not surprising since the family of delocalized trial states is built up from localized functions that appear to incorporate only small polaron structure—indeed, the emergence of a large polaron structure from such states can be viewed as one of the successes of the method—but there appear to be problems with the strong-coupling regime as well; though convergence toward small polaron structure at strong coupling is expected and observed, the *suddenness* with which the asymptotic form is approached above the self-trapping transition must be considered suspect.

Since we have implemented the method numerically making none of the simplifying assumptions commonly made, the root of all these difficulties certainly lies in the form of the variational trial state, and the route to their resolution therefore lies in an appropriate generalization. A successful generalization should significantly ''heal'' the rampant discontinuities associated with self-trapping, improve the quality of the variational bands at higher momenta, and reveal more structure in all polaron states, including those of the strong coupling regime. In the succeeding work, we implement such a generalization by building up delocalized trial states from localized functions explicitly incorporating a large polaron as well as a small polaron structure from the outset; this work follows the method originally proposed by Toyozawa.

ACKNOWLEDGMENT

[1] R. E. Merrifield, J. Chem. Phys. **40**, 4450 (1964).

[2] Yang Zhao, Doctoral thesis, University of California, San Diego, 1994.

[3] Y. Zhao, D.W. Brown, and K. Lindenberg (unpublished).

[4] Yutaka Toyozawa, Prog. Theor. Phys. **26**, 29 (1961).

[5] Y. Toyozawa, in *Polarons and Excitons*, edited by C. G. Kuper and G. D. Whitfield (Plenum, New York, 1963), pp. 211–232.

[6] Y. Toyozawa, in *Relaxation of Elementary Excitations*, edited by R. Kubo and E. Hanamura (Springer-Verlag, Heidelberg-New York, 1980).

[7] Sighart F. Fischer, in *Organic Molecular Aggregates*, Springer Series in Solid-State Sciences, Vol. 49, edited by P. Reineker, H. Haken and H. C. Wolf (Springer-Verlag, Berlin, 1983), pp. 107–119.

[8] Gerd Venzl and Sighart F. Fischer, J. Chem. Phys. **81**, 6090 (1984).

[9] Gerd Venzl and Sighart F. Fischer, Phys. Rev. B **32**, 6437 (1985).

[10] Bernhard Schopka, Doctoral thesis, Technische Universität München, 1991.

[11] S. I. Pekar, Journ. Phys. USSR **10**, 341 (1946).

[12] S. I. Pekar, Zh. Eksp. Theor. Fiz. **16**, 335 (1946).

[13] L. D. Landau and S. I. Pekar, Zh. Eksp. Teor. Fiz. **18**, 419 (1948).

[14] S. I. Pekar, *Untersuchungen Über die Elektronentheorie der Kristalle* (Akademie-Verlag, Berlin, 1954).

[15] A. S. Davydov, Phys. Stat. Sol. **36**, 211 (1969).

[16] A. S. Davydov and N. I. Kislukha, Phys. Stat. Sol. b **59**, 465 (1973).

[17] A. S. Davydov and N. I. Kislukha, Zh. Eksp. Teor. Fiz. **71**, 1090 (1976) [Sov. Phys. JETP **44**, 571 (1976)].

[18] A. S. Davydov, Phys. Scr. **20**, 387 (1979).

[19] M. J. Skrinjar, D. V. Kapor, and S. D. Stojanovic, Phys. Rev. A **38**, 6402 (1988).

[20] Q. Zhang, V. Romero-Rochin, and R. Silbey, Phys. Rev. A **38**, 6409 (1988).

[21] D. W. Brown and Z. Ivic, Phys. Rev. B **40**, 9876 (1989-I).

[22] Z. Ivic and D. W. Brown, Phys. Rev. Lett. **63**, 426 (1989).

[23] X. Wang, D. W. Brown, and K. Lindenberg, Phys. Rev. Lett. **62**, 1796 (1989).

[24] D. W. Brown, K. Lindenberg, and X. Wang, in *Davydov's Soliton Revisited: Self-Trapping of Vibrational Energy in Protein*, NATO ASI Series B: Physics, edited by P. Christiansen and A. C. Scott (Plenum, New York, 1990), Vol. 243, pp. 63–82.

[25] X. Wang, D. W. Brown, and K. Lindenberg, in Ref. 24, pp. 83–98.

[26] T. Holstein, Ann. Phys. NY **8**, 325 (1959).

[27] T. Holstein, Ann. Phys. NY **8**, 343 (1959).

[28] B. Gerlach and H. Lowen, Phys. Rev. B **35**, 4291 (1987).

[29] B. Gerlach and H. Lowen, Phys. Rev. B **35**, 4297 (1987).

[30] H. Lowen, Phys. Rev. B **37**, 8661 (1988).

[31] B. Gerlach and H. Lowen, Rev. Mod. Phys. **63**, 63 (1991).

[32] G. H. Wannier, Phys. Rev. **52**, 191 (1937).

[33] W. Kohn, Phys. Rev. **115**, 809 (1959).

[34] G. Weinreich, *Solids: Elementary Theory for Advanced Students* (Wiley, New York, 1965).

[35] O. Madelung, *Introduction to Solid-State Theory* (Springer-Verlag, New York, 1978).

[36] D. W. Brown, *Nonlinear Excitations in Biomolecules* (Centre de Physique des Houches, 1995), Vol. 2, p. 279.

[37] D. W. Brown, *Proceedings of the SPIE* (The International Society for Optical Engineering, 1995), Vol. 2526, p. 40.